Investigation and Simulation on Magnet Hysteresis Properties of Magneto-Rheological Fluid

Jianbin Zeng, Youguang Guo, *Senior Member, IEEE,* and Jianguo Zhu, *Senior Mem IEEE*

***Abstract*—Magneto-rheological fluid (MRF) materials are used in many devices as smart materials. However, the application of this material is limited to damper or vibration absorber because of the lack of understanding of its magnetic hysteresis properties. This paper systematically presents our recent investigation and simulation on the magnetic hysteresis properties of MRF materials. The measurement of its magnetic hysteresis property was accomplished by using a two-dimensional single sheet tester with an MRF sample container. An extended large-scale atomic/molecular massive parallel simulator (LAMMPS), which is combined with Stoner-Wohlfarth hysteresis model, was employed for simulating the magnetic hysteresis properties of MRF material. The measurement and simulation results are compared, analyzed and discussed. The results will be useful for modeling of magnetic hysteresis properties of MRF materials.**

***Index Terms*—Magnetic hysteresis, Magneto-rheological fluid, Magnetic field measurement, Magnetization**

I. Introduction

Magnetorheological fluid (MRF) is a type of material with magnetic particles in a carrier fluid, usually a type of oil. When it is subjected to a magnetic field, the fluid increases its apparent viscosity greatly to the point of becoming a viscoelastic solid. Importantly, the yield stress of the fluid in its active ("on") state can be controlled very accurately by varying the magnetic field intensity. The upshot is that the ability to transmit force can be controlled with an electromagnetic field. This promising feature makes MRF smart, simple, quiet and capable of a rapid interface between an electronic control system and a mechanical system. MRF materials have been widely used in various devices as “smart” materials [1-4]. However, the properties and mechanism of MRF materials have not been understood deeply, so their application in industry is still limited to damper or vibration absorber [5-10]. In recent years research work has been carried out on the property characterization of the MRF materials, followed by laboratory experiments and applications in other devices [11-16].

In order to describe the inherent behavior of the device, such as the hysteresis characteristics of the materials and associated devices, some mathematical models were proposed. However, these models cannot explain the magneto-rheological mechanism in generating the device forces. The effects of dynamic behavior, nonlinear and vector characteristics of MRF materials were not taken into account in these models. Therefore, the magnetic property investigation and measurement of MRF are very important to deeply understand the magneto-rheological mechanism, and then establish mathematical models involving the magnetic hysteresis behavior and vector magnetization.

It is noted that the molecular dynamic simulation is an efficient method to investigate the micro-scale suspension behaviors of magnetorheological fluid. The current simulations, however, mostly focus on the process of aggregation and micro-structure of magnetorheological fluid under constant magnetic field [17]. The simulation of magnetic hysteresis property and micro-structure of MRF material have been rarely reported. In order to simulate the magnetic property of MRF material, an open source molecular dynamic simulation software package, extended large-scale atomic/molecular massive parallel simulator (LAMMPS), was employed and modified.

Stoner-Wohlfarth model is a widely used model for the magnetization of single-domain ferromagnets. It is widely used for modeling small particle material in various applications [18]. Because the size of the ferromagnetic particles of MRF material is less than 10 micrometers, they could be treated approximately as single-domain particles. Hence, the Stoner-Wohlfarth magnetic hysteresis model was employed for the calculation of magnetic moment of ferromagnetic particles.

In this paper, the magnetic property of a kind of MRF material manufactured by Lord Ltd. USA, was measured under alternating and two-dimensional rotating magnetic fields by an

Manuscript received Month xx, 2xxx; revised Month xx, xxxx; accepted Month x, xxxx. This work was supported in part by the Natural Science Foundation of Fujian Province, China under Grant 2016J01747 and in part by the Xiamen University of Technology High Level Talents Projects under Grant YKJ15021R.

Jianbin Zeng is with the High-voltage Key Laboratory of Fujian Province, Xiamen University of Technology, Xiamen 361024, China (Phone: +86-592-62910-57; Fax: +86-592-6291305; E-mail: Jianbin.Zeng@xmut.edu.cn).

Youguang Guo and Jianguo Zhu are with the Faculty of Engineering and Information Technology, University of Technology Sydney, Australia (E-mails: Youguang.Guo-1@uts.edu.au; Jianguo.Zhu@uts.edu.au)

upgraded two-dimensional single sheet tester (2D-SST). The magnetic hysteresis property of this MRF material was also simulated by LAMMPS. Both measurement and simulation results are presented, compared and discussed. The results will be useful for modeling the magnetic hysteresis properties of MRF materials.

II. Theory

When an applied magnetic field is presented, the ferro-magnetic particles are affected by elastic force of matrix, gravity force of itself and magnetic force between particles. A schematic diagram of the i^{th} particle subjected to external forces is shown in Fig. 1 and its position is governed by the following Langevin equation

$$m\frac{\partial^2 r_i}{\partial t^2} = F_h + \sum_{j\neq i} F_m(r_{ij}) + F_w + F_B + F_g \quad (1)$$

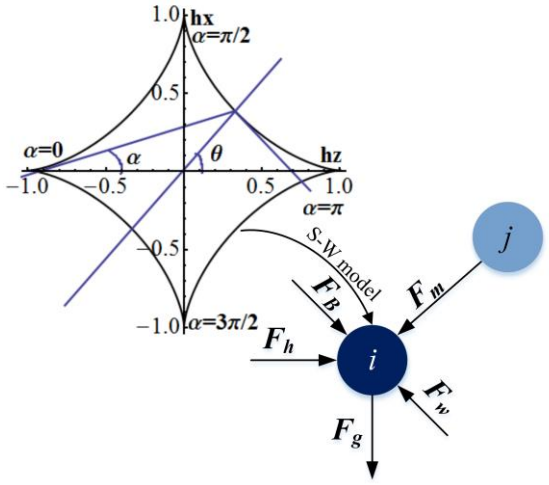

Fig. 1. Schematic diagram of the i^{th} particle subjected to external forces [16]

where $\boldsymbol{r_i}$ is the position vector and $\boldsymbol{r_{ij}}$ is the distance vector between the i^{th} and j^{th} particles. F_h denotes the hydrodynamic Stokes force [19]. F_m is the interaction force between the i^{th} and j^{th} particles. The symbol F_w denotes the interaction force between particles and boundaries. In this simulation, the periodic boundary conditions are applied. F_B is the fluctuating Brownian force and F_g is the gravity force of the i^{th} particle.

Magnetic particles are treated as magnetic dipoles in this paper. Therefore, the term F_m denoting the magnetic dipole interaction force between particles i and j, may be written as

$$F_m(r_{ij}) = F_d^0\left(\frac{r_{min,ij}}{r_{ij}}\right)\left[\vec{r}\left(\vec{m}_i\cdot\vec{m}_j\right) + \vec{m}_i\left(\vec{r}\cdot\vec{m}_j\right) + \vec{m}_j\left(\vec{r}\cdot\vec{m}_i\right) - 5\vec{r}\left(\vec{r}\cdot\vec{m}_i\right)\left(\vec{r}\cdot\vec{m}_j\right)\right] \quad (2)$$

where $\vec{m}_i$ and $\vec{m}_j$ are the unit vectors of magnetic moment of the i^{th} and j^{th} particles. $\vec{r}$ is the unit vector of center-to-center distance vector $\boldsymbol{r_{ij}}$ and $r_{min,ij} = a_i + a_j$ is the minimum sphere distance between two particles with radii a_i and a_j; $\boldsymbol{r_{ij}} = |\boldsymbol{r_j} - \boldsymbol{r_i}|$; and F_d^0 denotes the magneto-static force and takes the form

$$F_d^0 = \frac{3\mu_0\mu_c m_i m_j}{4\pi r^4_{min,ij}} \quad (3)$$

where $\mu_0 = 1.256e-7$ N/A is the vacuum permeability, μ_c is the relative permeability (with respect to the vacuum) of the matrix material, and m_i and m_j are the dipole moments of particles *i* and *j*, respectively [20].

For the magnetic property simulation of this material, the magnetic particles are treated as single domain particles. Hence, as shown in Fig. 1, a Stoner-Wohlfarth hysteresis model was applied on each particle, by which not only the nonlinear effect of magnetic property but also the magnetic hysteresis of this material could be considered in the simulation.

III. Experimental and Simulation

A. Magnetic hysteresis property measurement on MRF material

A 2D single sheet tester (2D-SST) [21] was upgraded to study the hysteresis properties of the MRF materials at the Centre for Electrical Machines and Power Electronics, University of Technology Sydney. Fig. 2 shows the schematic diagram of the whole testing system and the photo of 2D-SST.

The magnetic field used to magnetize the MRF materials is generated by two groups of electromagnets which are arranged along the X and Y axes, respectively. The excitation current was

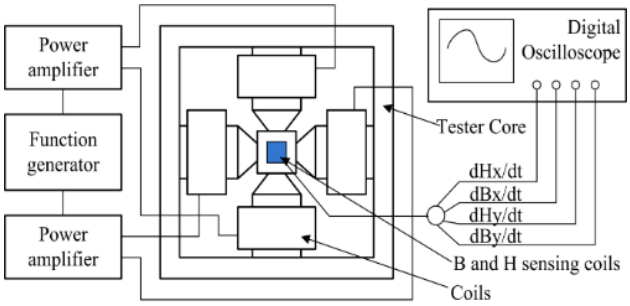

(a)

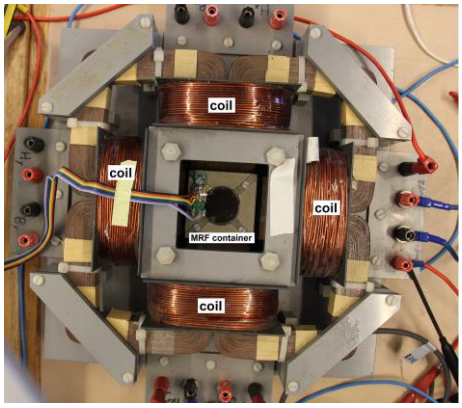

(b)

Fig. 2. (a) Schematic illustration, and (b) entity of the 2D single sheet tester

supplied by a power amplifier which has two output channels. The original waveform signal, which was the input of the power amplifier, was generated by a function generator. By varying the waveform signal, e.g. magnitude and/or phase, any combination of one- or two-dimensional magnetic field can be obtained, such as alternating magnetic flux density inclined at a specified angle from the X or Y axis, and circularly or elliptically rotating magnetic flux density. Various ***B*** loci in the sample, such as circles and ellipses, could be obtained by controlling magnitude and/or phase angle of output waveform of function generator. A group of circular ***B*** loci and corresponding ***H*** loci, shown in Fig. 3, have validated that the SST tester works well.

A square MRF sample container was placed in the center of SST tester, as shown in Fig. 2(b), which was designed for the measurement. The container was made of nonmagnetic Plexiglas material with four mild steel magnetic poles embedded along the four sides. The length of each edge is 54 mm. To improve the measurement precision, the MRF container was designed as sandwich structure. The top and bottom sections were separated by a middle partition with 1 mm thickness.

The magnetic field intensity sensing coil (H-coil) and flux density coils (B-coils) were fabricated to be small and thin to improve the measurement accuracy. The H-coil has two orthogonal thin windings so that it could measure both Hx and Hy components. The coil was embedded in the center of the partition and separated from the MRF sample by a 10 μm thickness plastic sheet. Eight B-coils were placed at the inner surface of the container, so that the flux densities along x- and y- directions could be measured. The H-coil and B-coil were calibrated in a long solenoid to obtain accurate coil coefficients. The positions of sensing coils are illustrated in Fig. 4. In this configuration, the H vectors were measured by the H-coils (#9 in Fig. 4), and the B vectors were measured by four pairs of small annular B-coils, that is, 1-3, 5-7 pairs measuring the x-direction and 2-4 and 6-8 pairs measuring the y-direction.

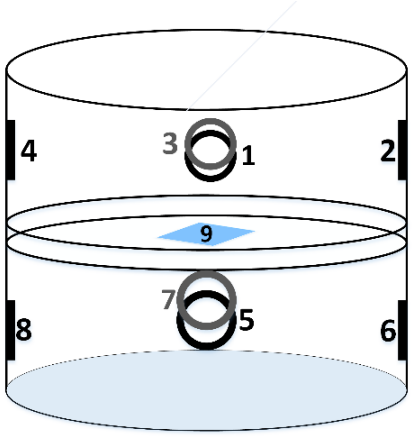

Fig. 4 Position of H sensing coils and B sensing coils.

B. Theory of measurement and calibration of sensing coils

The surface magnetic field strength along one axis, e.g. the x-axis or the y-axis, can be computed from the induced output voltage of the coil along that axis:

$$H_i = \frac{1}{\mu_o K_{Hi}} \int V_{Hi} dt \ (i = x, y) \tag{4}$$

where V_{Hi} is the output voltage of the coil, μ_o the permeability of air, and K_{Hi} the coil coefficients, which are determined by the calibration solenoid as K_{Hx}=0.00109, K_{Hy}=0.00147. The detail results are listed in Tables I and II, where I is the excitation current (15 Hz) input to the solenoid, BI is the magnetic flux density measured at the center of solenoid and H_m is the magnetic field intensity computed from BI. All the parameters are in RMS values.

TABLE I
H SENSING COIL COEFFICIENTS ON X AXIS

I(A)	*BI(T)*	*Hm(A/m)*	*VHx(V)*	*KHx*
3.005	0.00449	3575.637	0.00063	0.00112
4.243	0.00630	5019.108	0.00087	0.00110
5.233	0.00777	6187.102	0.00104	0.00107
6.116	0.00911	7250.796	0.00120	0.00105
7.036	0.01050	8357.484	0.00140	0.00106
6.081	0.00903	7185.510	0.00123	0.00108
5.162	0.00766	6100.318	0.00106	0.00110
4.172	0.00620	4939.490	0.00085	0.00109
2.970	0.00441	3507.962	0.00063	0.00114
		Average KHx		0.00109

TABLE II
H SENSING COIL COEFFICIENTS ON Y AXIS

I(A)	*BI(T)*	*Hm(A/m)*	*VHy*	*KHy*
3.005	0.00449	3578.025	0.00084	0.00149
4.243	0.00630	5013.535	0.00116	0.00147
5.233	0.00776	6177.548	0.00143	0.00147
6.116	0.00910	7243.631	0.00165	0.00144
7.036	0.01050	8356.688	0.00190	0.00144
6.081	0.00904	7194.268	0.00165	0.00145
5.162	0.00767	6107.484	0.00141	0.00146
4.172	0.00620	4939.490	0.00116	0.00149
2.970	0.00442	3515.924	0.00082	0.00148
		Average KHy		0.00147

The flux density on one axis can be calculated by

$$B_i = \frac{1}{N_{Bi} A_{Bi}} \int V_{Bi} dt \ \ (i = x, y) \tag{5}$$

where N_{Bi} is the number of turns, A_{Bi} the cross-sectional area, and V_{Bi} the induced terminal voltage of the B-coil on the axis. The coefficients $K_{Bi}=N_{Bi}A_{Bi}$ can also be determined by the

calibration solenoid as K_{Bx}=0.00143, K_{By}=0.00138. The detail results are listed in Tables III and IV. All the parameters are in RMS values.

TABLE III
B SENSING COIL COEFFICIENTS ON X AXIS

I(A)	*BI(T)*	*VBx(V)*	*KBx*
3.005	0.00455	0.00168	0.00147
4.243	0.00640	0.00230	0.00143
5.303	0.00788	0.00280	0.00141
6.187	0.00922	0.00328	0.00142
7.142	0.01062	0.00378	0.00142
6.152	0.00913	0.00327	0.00143
5.233	0.00775	0.00280	0.00144
4.207	0.00627	0.00225	0.00143
2.970	0.00446	0.00160	0.00143
	Average KBx		0.00143

TABLE IV
B SENSING COIL COEFFICIENTS ON Y AXIS

I(A)	*BI(T)*	*Vby(V)*	*KBy*
3.005	0.00450	0.00158	0.00140
4.243	0.00631	0.00219	0.00138
5.233	0.00777	0.00268	0.00137
6.116	0.00910	0.00314	0.00137
7.071	0.01053	0.00361	0.00136
6.081	0.00904	0.00311	0.00137
5.162	0.00768	0.00265	0.00137
4.172	0.00621	0.00215	0.00138
2.934	0.00441	0.00155	0.00140
	Average KBy		0.00138

C. MRF material sample

A kind of MRF, MRF-132DG, manufactured by LORD Ltd. USA, was used in the magnetic hysteresis property investigation. Table V lists the typical properties of the material.

TABLE VI
TYPICAL PROPERTIES OF MRF-132DG

Appearance	Dark Gray Liquid
Viscosity①, Pa @ 40°C (104°F) Calculated as slope 800-1200 sec^{-1}	0.092 ± 0.015
Density g/cm^3	2.98-3.18
Solids Content by Weight, %	80.98
Flash Point②, °C (°F)	>150 (>302)
Operating Temperature, °C (°F)	-40 to +130 (-40 to +266)
Relative permeability	≈ 4.24

① The viscosity of a fluid is a measure of its resistance to gradual deformation by shear stress or tensile stress. For liquids, it corresponds to the informal concept of "thickness".
②The flash point of a volatile material is the lowest temperature at which vapors of a fluid will ignite.

D. Simulation

For simulating the magnetic hysteresis properties of MRF materials, an extended large-scale atomic/molecular massive parallel simulator (LAMMPS) was employed. It provides not only an embedded routine for large-scale and 3D Brownian dynamic simulation but also an extensive library of potential functions and force fields. In this paper, the function of the magnetic force and Stoner-Wohlfarth hysteresis model was added to this software package. Hence, it can not only simulate the aggregation of magnetic particle of MRF materials under applied magnetic field, but also the magnetic hysteresis properties of MRF materials.

A particle system which contains 4000 particles, shown in Fig. 5, was used to simulate the aggregation structure and magnetic hysteresis properties of MRF material. The aggregation structures of MRF material under 1D alternating and 2D rotating applied magnetic field are shown in Fig. 5(a) and Fig. 5(b), respectively. In this simulation, each particle was applied by a Stoner-Wohlfarth magnetic hysteresis model and the orientation of easy axis was set randomly. The magnetization-status of each particle, such as orientation of

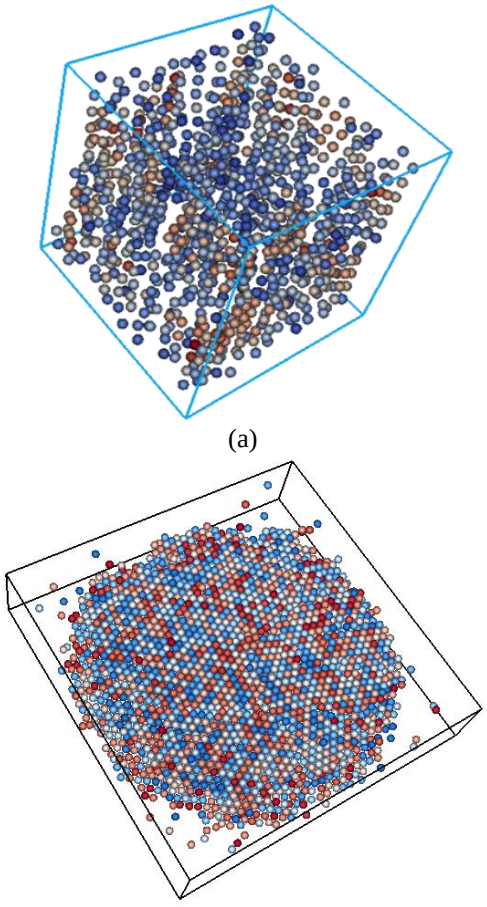

(a) (b)

Fig. 5. Aggregation structure of particles in MRF material under (a) 1D alternating, and (b) 2D-rotating applied magnetic field

easy axis, intensity of magnetization (***M***) and intensity of applied magnetic field (***H***), was updated and recorded in each time step. Various ***M*** could be obtained by accumulating the ***Ms*** of all the particles.

IV. Results and Discussion

A. Magnetic hysteresis property under 1D alternating applied field

Fig. 6 illustrates the measured (solid line) and simulated (solid line with circular symbols) H-B hysteresis loop of MRF material with 15 Hz, 1D alternating applied magnetic field. The measured remanence is 0.006 T, the coercivity is 0.038 kA/m, and the relative permeability is about 4.56, which is not large due to particle separation and strong demagnetization field. The relative permeability is consistent with the data provided by manufacturer. The simulated remanence is 0.009 T, the coercivity is 0.12 kA/m, and the relative permeability is 4.43.

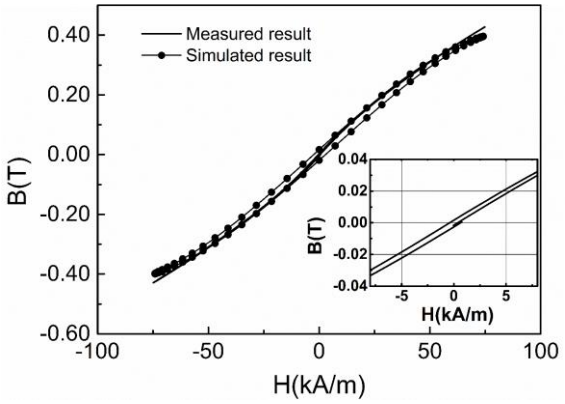

Fig. 6. Measured and simulated H-B loop of MRF material under 15 Hz, 1D alternating applied magnetic field. The loop in solid line is the measured result and the loop with the dotted line is the simulated result.

B. Magnetic hysteresis property under 2D rotating applied magnetic field

In the measuring of magnetic hysteresis property under 2D rotating applied magnetic field, people often measure the H loci under circular ***B*** loci because the ***B*** loci is easier to be controlled as a circular shape than ***H*** loci. Fig. 7 shows a series of controlled circular ***B*** loci (a) and corresponding ***H*** loci (b) at 15 Hz. It can be seen from the ***B*** and ***H*** loci that the sample shows isotropic characteristic when it is subjected to circular magnetic fields. The slight distortions of ***H*** loci may be caused by magnetic coupling between x- and y-axis poles of the tester because the particles aggregated between the neighbor poles.

Fig. 8 illustrates the simulation of a series of controlled circular ***H*** loci (b) and corresponding ***B*** loci (a) at 15 Hz. It can be seen from the ***B*** and ***H*** loci that the simulation results show isotropic characteristic which are similar to the measured results. For simulation, the magnetic field intensity ***H*** was set before running the simulation, so the shape of ***H*** loci could be controlled as circle easily. On the other hand, the shape of ***B*** loci cannot be controlled as circles easily because the ***B*** loci are the output of particle system and affected by the complex

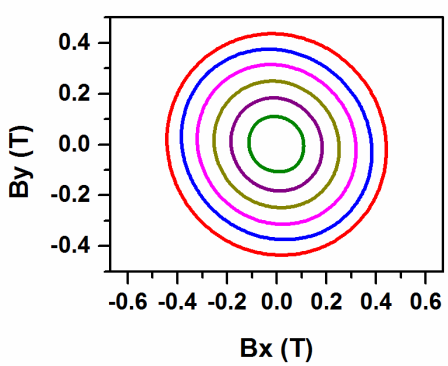

(a)

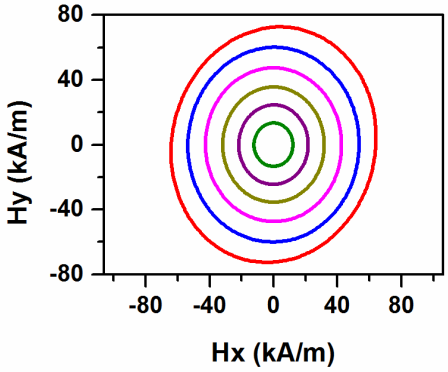

(b)

Fig. 7. Circular ***B*** loci (a) and corresponding ***H*** loci (b) at 15 Hz

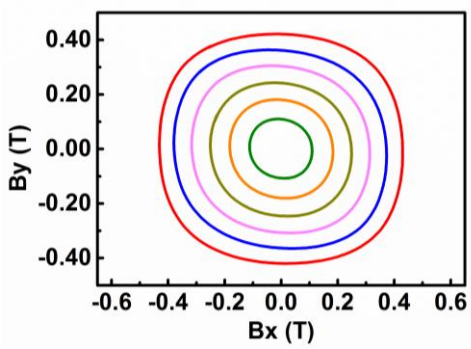

(a)

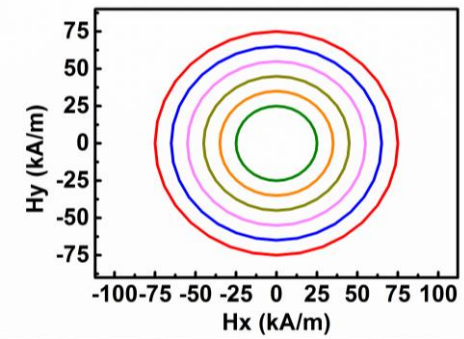

(b)

Fig. 8. Circular ***H*** loci (b) and corresponding ***B*** loci (a) simulated at 15 Hz, rotating magnetic field

interaction of $\boldsymbol{B}$ among particles.

V. Conclusion

Some research results on magnetic hysteresis property of MRF material were presented in this paper. The magnetic hysteresis property of this material under 1D alternating and 2D rotating applied magnetic fields was measured and investigated. A molecular dynamic simulation method, which combines Stoner-Wohlfarth magnetic hysteresis model and molecular dynamic simulation, was applied successfully to simulate the aggregation structure and the hysteresis property of MRF material. The simulation results illustrate the different aggregation structure of MRF material under 1D alternating and 2D rotating applied magnetic field. This enables us to reveal the relationship of magnetic hysteresis properties between microscopic ferromagnetic particle and macroscopic MRF material and it is also possible to propose a new magnetic hysteresis model based on the work of this paper.

References

[1] J. de Vicente, D. J. Klingenberg, and R. Hidalgo-Alvarez, "Magnetorheological fluids: a review," *Soft Matter.*, vol. 7, pp. 3701-3710, 2011.

[2] I. Sahin, T. Engin, and S. Cesmeci, "Comparison of some existing parametric models for magnetorheological fluid dampers," *Smart Materials & Structures*, vol. 19, pp. 3–7, Mar. 2010.

[3] C. A. Smith and E. H. Anderson, "Passive damping by smart materials - analysis and practical limitations," *Passive Damping*, vol. 2445, pp. 136-148, 1995.

[4] C. Ekwebelam and H. See, "Microstructural investigations of the yielding behaviour of bidisperse magnetorheological fluids," *Rheologica Acta*, vol. 48, pp. 19-32, 2009.

[5] A. Boczkowska, S. Awietjan, T. Wejrzanowski, and K. Kurzydłowski, "Image analysis of the microstructure of magnetorheological elastomers," *Journal of Materials Science*, vol. 44, pp. 3135-3140, 2009.

[6] S. Krishnamurthy, A. Yadav, P. Phelan, R. Calhoun, A. Vuppu, A. Garcia, and M. Hayes, "Dynamics of rotating paramagnetic particle chains simulated by particle dynamics, Stokesian dynamics and lattice Boltzmann methods," *Microfluidics and Nanofluidics*, vol. 5, pp. 33-41, 2008.

[7] K. Yao, Z. Hou, X. Zhao, and X. Tian, "Circuit design of semi-active controller for MR damper," in *Proc. Int. Conf. on Intelligent Computation Technology and Automation (ICICTA)*, 2010, pp. 929-931.

[8] H Böse, J Ehrlich, and A-M Trendler, "Performance of magneto-rheological fluids in a novel damper with excellent fail-safe behavior," *Journal of Physics: Conference Series*, vol. 149, p. 012039, 2009.

[9] A. Rodriguez Tsouroukdissian, F. Ikhouane, J. Rodellar, and N. Luo, "Modeling and identification of a small-scale magnetorheological damper," *Journal of Intelligent Material Systems and Structures*, vol. 42, pp. 21–25, 2008.

[10] H. S. Hu, H. Wang, S. X. Qian, and L. J. Zhang, "Research on the hardware-in-the-loop simulation of magnetorheological damper subjected to impact load," in *Proc. 2008 IEEE International Conference on Automation and Logistics*, vols. 1-6, pp. 1668-1673, 2008.

[11] F. Zhang Sai and Y. Liu, "Disc shaped high-torque-MRF-clutch design," in *Proc. Int. Conf. Computer Application and System Modeling (ICCASM)*, pp. V13-374-V13-377.

[12] C. Wu, W. Wang, H. Shi, and W. Zhang, "Research on the stability of vehicle suspension excited by the road surface profile," *in Proc. 2nd Int. Conf. Computer Modeling and Simulation*, , pp. 164-168.

[13] K. H. Kim, Y. J. Nam, R. Yamane, and M. K. Park, "Smart mouse: 5-DOF haptic hand master using magneto-rheological fluid actuators," *Journal of Physics: Conference Series*, vol. 149, p. 012062, 2009.

[14] Z. Tian Zu, F. Hou You, and N. Wang Nan, "The design of magnetic circuit and magnetic field finite element analysis of a double discs magnetorheological clutch," in *Proc. Int. Conf. Mechatronics and Automation (ICMA)*, 2010, pp. 1732-1737.

[15] S. Salzman, H. J. Romanofsky, S. D. Jacobs, and J. C. Lambropoulos, "Surface–texture evolution of different chemical-vapor-deposited zinc sulfide flats polished with various magnetorheological fluids," *Precision Engineering*, vol. 43, pp. 257-261, 2016.

[16] F. Li, P. Xu, X. Sui, and F. Zhou, "Evaluation of the quality for sheet deep drawing using a magnetorheological fluid (MRF)," *Modern Physics Letters B*, vol. 29, p. 1550141, 2015.

[17] Y. B. Peng, R. Ghanem, and J. Li, "Investigations of microstructured behaviors of magnetorheological suspensions," *Journal of Intelligent Material Systems and Structures*, vol. 23, pp.1351-1370, 2012.

[18] E. C. Stoner and E. P. Wohlfarth, "A mechanism of magnetic hysteresis in heterogeneous alloys," *IEEE Trans. Magn.*, vol. 27, pp. 3475-3518, 1991.

[19] D. J. Klingenberg, F. van Swol, and C. F. Zukoski, "Dynamic simulation of electrorheological fluids," *J. Chem. Phys.*, vol. 91, p. 7888, 1989.

[20] K. W. Yung, P. B. Landecker, and D. D. Villani, "An analytic solution for the force between two magnetic dipoles," *Magnetic and Electrical Separation*, vol. 9, pp. 39-52, 1998.

[21] J. B. Zeng, Y. G. Guo, Y. C. Li, J. G. Zhu, and J. C. Li, "Two-dimensional magnetic property measurement for magneto-rheological elastomer," *J. Applied Physics*, vol. 113, pp. 17A919-1-3, 2013.

Jianbin Zeng was born in Liancheng county, Fujian Province, China. He received the PhD Degree in electrical engineering from Shenyang University of Technology (SUT), China in 2011.

He worked in the Department of Electrical Engineering of SUT as research assistant from 1999 to 2006. He was an associate lecturer of Biomedical Engineering at the School of Electrical Engineering, SUT from May 2006 to Jun 2007, and was a Lecturer from July 2007 to December 2010. From January 2011 to March 2014, He worked in the Centre for Electrical Machines and Power Electronics, Faculty of Engineering and Information Technology, University of Technology Sydney (UTS), Australia. Since May 2015, he has been working at the School of Electrical Engineering & Automation, Xiamen University of Technology, China.

Youguang Guo (S'02-M'05-SM'06) was born in Hubei, China in 1965. He received the B.E. degree from Huazhong University of Science and Technology, China in 1985, the M.E. degree from Zhejiang University, China in 1988, and the Ph.D. degree from University of Technology Sydney (UTS), Australia in 2004, all in electrical engineering. He is currently an associate professor at the School of Electrical, Mechanical and Mechatronic Systems, UTS.

His research areas include measurement and characterization of magnetic properties of magnetic materials, numerical analysis of electromagnetic field, electrical machine design and optimization, power electronic drives and motor control.

Jianguo Zhu (S'93–M'96–SM'03) received the B.E. degree from Jiangsu Institute of Technology, Zhenjiang, China, in 1982, the M.E. degree from Shanghai University of Technology, Shanghai, China, in 1987, and the Ph.D. degree from the University of Technology Sydney (UTS), Sydney, Australia, in 1995, all in electrical engineering.

He is currently a Professor of electrical engineering and the Head of the School of

Electrical, Mechanical and Mechatronic Systems with the UTS. His current research interests include electromagnetics, magnetic properties of materials, electrical machines and drives, power electronics and green energy systems.